

Relativistic coupled-cluster theory analysis of unusually large correlation effects in the determination of g_j factors in Ca^+

B. K. Sahoo^a * and Pradeep Kumar^{a,b}

^a*Atomic, Molecular and Optical Physics Division,
Physical Research Laboratory, Navrangpura, Ahmedabad-380009, India and*

^b*Indian Institute of Technology Gandhinagar, Ahmedabad, India*

(Dated: Recieved date; Accepted date)

We investigate roles of electron correlation effects in the determination of the g_j factors of the $4s\ ^2S_{1/2}$, $4p\ ^2P_{1/2}$, $4p\ ^2P_{3/2}$, $3d\ ^2D_{3/2}$, and $3d\ ^2D_{5/2}$ states, representing to different parities and angular momenta, of the Ca^+ ion. Correlation contributions are highlighted with respect to the mean-field values evaluated using the Dirac-Hartree-Fock method, relativistic second order many-body theory, and relativistic coupled-cluster (RCC) theory with the singles and doubles approximation considering only the linear terms and also accounting for all the non-linear terms. This shows that it is difficult to achieve reasonably accurate results employing an approximated perturbative approach. We also find that contributions through the non-linear terms and higher-level excitations such as triple excitations, estimated perturbatively in the RCC method, are found to be crucial to attain precise values of the g_j factors in the considered states of Ca^+ ion.

PACS numbers: 31.30.js;31.15.A-;31.15.vj;31.15.bw

I. INTRODUCTION

Spectroscopic studies of the singly ionized calcium (Ca^+) ion is of immense interest to both the experimentalists and theoreticians on many scientific applications. Particularly, this ion is under consideration for a number of high precision experimental studies such as in the atomic clock [1, 2], quantum computation [3–5], testing Lorentz symmetry violation [6], etc. A number of theoretical investigations have also been carried out in the determination of different physical quantities by employing varieties of many-body methods [7–14], which demonstrate successfully achieving most of these properties meticulously compared to the experimental results.

On the otherhand, there have been attempts to determine Lande g_j factors in the atomic systems to ultra-high accuracy [7, 15–17]. The main motivation of these studies was to test validity of both the theories and measurements. Mostly, atomic systems with few electrons are being considered in these investigations aiming to find out role of higher order quantum electro-dynamics (QED) effects [17]. In these systems, both the QED and electron correlation effects contribute at par to match the theoretical calculations with the experimental results. Comparatively, only few attempts have been made to reproduce the experimental values of the g_j factors to very high precision in the many-electron systems [7, 15]. In the neutral or singly ionized heavy atomic systems, the

electron correlation effects play the dominant roles for estimating the g_j factors of the atomic states accurately. However, none of the previous studies have demonstrated the roles of electron correlation effects explicitly arising through various physical effects in the determination of the total values of the g_j factors of the heavy atomic systems. Lindroth and Ynnerman had carried out such a rigorous investigation on the role of electron correlation effects to the corrections over Dirac value of the g_j factors of the ground states in the Li, Be^+ and Ba^+ atomic systems, which have a valence electron in the s orbital. They had employed a relativistic coupled-cluster (RCC) method and incorporated Breit interaction in their calculations and found that higher order correlation effects and Breit interaction play significant roles in achieving precise results. However, they had observed that lower order contributions are still dominant in the evaluation of the corrections over Dirac value of the g_j factors. Especially, they had observed that correlations due to all order core-polarization effects, arising through random-phase approximation (RPA) type of diagrams, in these calculations are crucial. A number of calculations have reported very accurate values of this quantity using multi-configuration Dirac-Fock (MCDF) method highlighting the importance of including the higher excited configuration state functions (CSFs) for their determinations [7, 18]. Shortcoming of this method is that it cannot explain roles of different electron correlation effects explicitly except giving a qualitative idea on their importance for incorporating to achieve precise results. Other points to be noted is that the MCDF method is a special case of the configuration interaction (CI) method. It is known

*Email: bijaya@prl.res.in

that a truncated CI method have size consistent and size extensivity problems [19, 20]. Moreover in practice, only the important contributing CSFs are being selected in this approach till the final results are achieved within the intended accuracies. In contrast, the truncated many-body methods formulated in the RCC theory framework are more capable of capturing the electron correlation effects rigorously than other existing atomic many-body methods and are also free from the size extensivity and size consistent problems owing to exponential ansatz of the wave functions [19, 20]. This is why RCC methods are generally termed as the golden tools for investigating roles of electron correlation effects in the spectroscopic studies. A number of properties in Ca^+ have been calculated employing the RCC methods in the singles and doubles approximation (CCSD method) [9–12, 21, 22]. From these studies, the CCSD method and its equivalent level of approximated RCC methods are proven to be capable of giving very accurate results in the atomic systems having similar configurations with Ca^+ . Thus, it would be interesting to learn how differently electron effects behave in the evaluation of the total values of the g_j factors of the ground state as well as of the excited states belonging to both the parities and higher orbital angular momenta of an alkali-like atomic system like Ca^+ . The present work is intended to demonstrate this by carrying out calculations of the g_j factors of the $4s^2S_{1/2}$, $4p^2P_{1/2}$, $4p^2P_{3/2}$, $3d^2D_{3/2}$, and $3d^2D_{5/2}$ states in the Ca^+ ion.

II. THEORY

The interaction Hamiltonian of an atomic electron when subjected to an external homogeneous magnetic field $\vec{\mathbf{B}}$ is given by [23]

$$\begin{aligned} H_{mag} &= ec \sum_i \vec{\alpha}_i \cdot \vec{\mathbf{A}}_i \\ &= -\frac{ec}{2} \sum_i \vec{\alpha}_i \cdot (\vec{\mathbf{r}}_i \times \vec{\mathbf{B}}), \end{aligned} \quad (1)$$

where e is the electric charge of the electron, c is the speed of light, $\vec{\alpha}$ is the Dirac operator, and $\vec{\mathbf{A}}$ is the vector field seen by the electron located at r due to the applied magnetic field. This interaction Hamiltonian can be expressed in terms of a scalar product as

$$\begin{aligned} H_{mag} &= -\frac{ec}{2} \sum_i (\vec{\alpha}_i \times \vec{\mathbf{r}}_i) \cdot \vec{\mathbf{B}} \\ &= i\frac{ec}{\sqrt{2}} \sum_i r_i \left\{ \vec{\alpha}_i \otimes \vec{\mathbf{C}}^{(1)} \right\}^{(1)} \cdot \vec{\mathbf{B}} \end{aligned} \quad (2)$$

with $C^{(1)}$ is the Racah coefficient of rank one.

Defining the above expression as $H_{mag} = \vec{\mathcal{M}} \cdot \vec{\mathbf{B}}$ with magnetic moment operator $\vec{\mathcal{M}} = \sum_{i,q=-1,0,1} \vec{\mu}_q^{(1)}(r_i)$, the Dirac value to the Lande g_j factor of a bound electron

in an atomic system can be given by

$$g_j^D = -\frac{1}{\mu_B} \frac{\vec{\mathcal{M}}}{\vec{\mathbf{J}}} \quad (3)$$

of a state with total angular momentum \mathbf{J} for the Bohr magneton $\mu_B = e\hbar/2m_e$ with mass of electron m_e . Thus, the g_j^D value for the state $|JM\rangle$ can be evaluated using the projection theorem as

$$g_j^D = -\frac{1}{2\mu_B} \frac{\langle J||\mathcal{M}||J\rangle}{\sqrt{J(J+1)(2J+1)}}, \quad (4)$$

with the corresponding single particle reduced matrix element of $\boldsymbol{\mu}^{(1)}$ given by

$$\begin{aligned} \langle \kappa_f || \boldsymbol{\mu}^{(1)} || \kappa_i \rangle &= -(\kappa_f + \kappa_i) \langle -\kappa_f || \mathbf{C}^{(1)} || \kappa_i \rangle \\ &\times \int_0^\infty dr r (P_f Q_i + Q_f P_i), \end{aligned} \quad (5)$$

where $P(r)$ and $Q(r)$ denote for the large and small components of the radial parts of the single particle Dirac orbitals, respectively, and κ are their relativistic angular momentum quantum numbers. It can be noted here that this expression is similar to the expression for determining the magnetic dipole hyperfine structure constant, in both the properties the angular momentum selection rule is restricted by the reduced matrix element of $C^{(1)}$, which is given as

$$\begin{aligned} \langle \kappa_f || \mathbf{C}^{(k)} || \kappa_i \rangle &= (-1)^{j_f+1/2} \sqrt{(2j_f+1)(2j_i+1)} \\ &\begin{pmatrix} j_f & k & j_i \\ 1/2 & 0 & -1/2 \end{pmatrix} \Pi(l_{\kappa_f}, k, l_{\kappa_i}), \end{aligned} \quad (6)$$

with

$$\Pi(l_{\kappa_f}, k, l_{\kappa_i}) = \begin{cases} 1 & \text{for } l_{\kappa_f} + k + l_{\kappa_i} = \text{even} \\ 0 & \text{otherwise,} \end{cases} \quad (7)$$

for the orbital momentum l_κ of the corresponding orbital having the relativistic quantum number κ .

The net Lande g factor of a free electron (g_f) with the QED correction on the Dirac value (g_D) can be approximately evaluated by [24]

$$\begin{aligned} g_f &\simeq g_D \times \left[1 + \frac{1}{2} \frac{\alpha_e}{\pi} - 0.328 \left(\frac{\alpha_e}{\pi} \right)^2 + \dots \right] \\ &\approx 1.001160 \times g_D, \end{aligned} \quad (8)$$

where α_e is the fine structure constant. From this analysis, the QED correction to the bound electron g_j factor can be estimated approximately by the interaction Hamiltonian as [25]

$$\Delta H_{mag} \approx 0.001160 \mu_B \beta \vec{\Sigma} \cdot \vec{\mathbf{B}}, \quad (9)$$

where β and $\vec{\Sigma}$ are the Dirac matrix and spinor, respectively. Following the above procedure, we can estimate

leading order QED correction to g_j by defining an operator $\Delta\vec{\mathcal{M}} = \sum_{i,q=-1,0,1} \Delta\vec{\mu}_q^{(1)}(r_i) = \sum_i \beta_i \vec{\Sigma}_i$ such as [18]

$$\Delta g_j^Q = 0.001160 \frac{\langle J || \Delta\vec{\mathcal{M}} || J \rangle}{\sqrt{J(J+1)(2J+1)}}. \quad (10)$$

The corresponding reduced matrix element of the $\Delta\mu_q^{(1)}(r_i)$ is given by

$$\begin{aligned} \langle \kappa_f || \Delta\mu^{(1)} || \kappa_i \rangle &= (\kappa_f + \kappa_i - 1) \langle -\kappa_f || \mathbf{C}^{(1)} || \kappa_i \rangle \\ &\times \int_0^\infty dr (P_f P_i + Q_f Q_i). \end{aligned} \quad (11)$$

Hence, the total g_j value of an atomic state can be evaluated as $g_j = g_j^D + \Delta g_j^Q$ and can be compared with the experimental value wherever available.

III. METHODS FOR CALCULATIONS

The considered states of Ca^+ have a common closed-core [$3p^6$] of Ca^{2+} with a valence orbital from different orbital angular momenta and parity. We have developed a number of relativistic many-body methods and have been employing them to calculate wave functions of a variety of atomic systems including in Ca^+ that have configurations as a closed-core and a valence orbital [9, 11, 21, 22, 26, 27]. Applications of these methods have proved that they are capable of giving rise very accurate results comparable with the experimental values. We apply some of these methods considering various levels of approximations to demonstrate how these methods are incapable of producing precise values of the g_j factors in Ca^+ . To find the reason for the same, the role of correlation effects at the lower and higher order contributions are investigated systematically. Special efforts have been made to estimate contributions from the leading triply excited configurations in the RCC theory framework adopting perturbative approaches to reduce the computational resources. For this purpose, we briefly discuss here the considered many-body methods and present results employing these methods to justify our above assessment.

To demonstrate various relativistic contributions systematically, we first perform calculations with the Dirac-Coulomb (DC) interaction and suppressing contributions from the negative orbitals. In this approximation, the atomic Hamiltonian is given by

$$\begin{aligned} H^{\text{DC}} &= \sum_i \Lambda_i^+ [c\vec{\alpha}_i \cdot \vec{p}_i + (\beta_i - 1)c^2 + V_{\mathcal{N}}(r_i)] \Lambda_i^+ \\ &+ \sum_{i,j>i} \Lambda_i^+ \Lambda_j^+ \frac{1}{r_{ij}} \Lambda_i^+ \Lambda_j^+, \end{aligned} \quad (12)$$

where $V_{\mathcal{N}}(r)$ is the nuclear potential and determined using the Fermi-charge distribution, $r_{ij} = |\vec{\mathbf{r}}_i - \vec{\mathbf{r}}_j|$ represents inter-electronic distance between the electrons located at i and j , and Λ^+ operator represents a projection

operator on to the positive energy orbitals. It is worth mentioning here is that the negative energy orbitals may contribute to quite significant, but it would be below the precision levels where the neglected electron correlation effects can also play dominant roles. That is the reason why we have not put efforts to account for these contributions in the present work.

It is found in the previous calculation for the ground state of Ca^+ , the frequency independent Breit interaction contributes sizably for the evaluation of the g_j factor [7]. We also estimate contributions due to this interaction by adding the corresponding interaction potential energy expression in the atomic Hamiltonian as given by

$$V_B(r_{ij}) = -\frac{\{\vec{\alpha}_i \cdot \vec{\alpha}_j + (\vec{\alpha}_i \cdot \hat{\mathbf{r}}_{ij})(\vec{\alpha}_j \cdot \hat{\mathbf{r}}_{ij})\}}{2r_{ij}}, \quad (13)$$

where $\hat{\mathbf{r}}_{ij}$ is the unit vector along $\vec{\mathbf{r}}_{ij}$.

Apart from estimating Δg_j^Q corrections to the g_j factors due to the QED effects, it can be expected that there would be corrections to the g_j^D values of the bound electrons from the modifications of the wave functions due to the QED effects. To estimate these corrections, we consider the lowest order QED interactions due to the vacuum potential (VP) and self-energy (SE) effects in the calculations of the wave functions of the bound electrons. The VP potential is considered as sum of the Uehling ($V_U(r)$) and Wichmann-Kroll ($V_{WK}(r)$) potentials, while the SE potential energy is evaluated as sum of the contributions from the electric and magnetic form-factors as were originally described in Ref. [28]. The considered expressions with the Fermi charge distribution are given explicitly in our previous work [27].

We first calculate the Dirac-Hartree-Fock (DHF) wave function of the [$3p^6$] configuration ($|\Phi_0\rangle$) using the above interactions in the atomic Hamiltonian. Then, the DHF wave function of a state of Ca^+ is constructed as $|\Phi_v\rangle = a_v^\dagger |\Phi_0\rangle$ with the respective valence orbital v of the state. To show higher relativistic contributions explicitly, we perform calculations considering the DC Hamiltonian, then including the Breit interaction with the DC Hamiltonian, then with QED corrections in the DC Hamiltonian and finally, incorporating both the Breit and QED interactions simultaneously with the DC Hamiltonian. The reason for carrying out calculations considering individual relativistic corrections separately and then including them together is that we had observed in our previous study as sometimes correlations among the Breit and QED interactions alter the results than when they are incorporated independently.

To investigate importance of electron correlation effects, we include them both in the lower order and all order many-body methods. In the lower order approximations, we employ the relativistic second order many-body perturbation theory (MBPT(2) method) and third order many-body perturbation theory (MBPT(3) method). In these approximations, we express the approximated atomic wave function as

$$|\Psi_v\rangle = (1 + \Omega_0^{(1)} + \Omega_v^{(1)}) |\Phi_v\rangle, \quad (14)$$

TABLE I: Electron attachment energies (in cm^{-1}) using relativistic many-body methods at different levels of approximations with the DC Hamiltonian. Higher order relativistic corrections from the Breit interaction and QED effects are quoted from the CCSD method considering them separately and including together (given as “Breit+QED”). Our final CCSD results are compared with the experimental values (mentioned as “Expt”) listed in the NIST database [30].

Method	$4s^2S_{1/2}$	$3d^2D_{3/2}$	$3d^2D_{5/2}$	$4p^2P_{1/2}$	$4p^2P_{3/2}$
DHF	91439.97	72617.49	72593.39	68036.82	67837.16
MBPT(2)	96542.41	83943.81	83372.99	71026.03	70654.06
LCCSD	96737.80	84564.90	84397.55	71101.05	70862.78
CCSD	95879.60	81695.19	81606.44	70603.50	70372.14
Relativistic corrections					
Breit	-7.42	37.98	53.15	-11.02	-3.70
QED	-5.68	2.11	2.52	0.02	0.66
Breit+	-13.09	40.08	55.67	-11.01	-3.05
QED					
Total	95866.51	81735.27	81662.11	70592.49	70369.09
Expt	95751.87(3)	82101.68	82040.99	70560.36	70337.47

in the MBPT(2) method and

$$|\Psi_v\rangle = (1 + \Omega_0^{(1)} + \Omega_v^{(1)} + \Omega_0^{(1)}\Omega_v^{(1)} + \Omega_0^{(2)} + \Omega_v^{(2)})|\Phi_v\rangle, \quad (15)$$

in the MBPT(3) method, where Ω_0 and Ω_v are known as wave operators. Here Ω_0 and Ω_v act over $|\Phi_0\rangle$ and $|\Phi_v\rangle$, respectively, to generate various CSFs in the perturbative approach. Amplitudes of these operators are determined by using the generalized Bloch’s equations [29] as

$$\langle\Phi_0^*|[\Omega_0^{(k)}, H_0]|\Phi_0\rangle = \langle\Phi_0^*|V_{es}(1 + \Omega_0^{(k-1)})|\Phi_0\rangle \quad (16)$$

and

$$\begin{aligned} \langle\Phi_v^*|[\Omega_v^{(k)}, H_0]|\Phi_v\rangle &= \langle\Phi_v^*|V_{es}(1 + \Omega_0^{(k-1)} + \Omega_v^{(k-1)})|\Phi_v\rangle \\ &\quad - \sum_{m=1}^{k-1} \langle\Phi_v^*|\Omega_v^{(k-m)}|\Phi_v\rangle E_v^{(m)}, \end{aligned} \quad (17)$$

where H_0 is the DHF Hamiltonian, $V_{es} = H - H_0$ is the residual potential, $|\Phi_0^*\rangle$ and $|\Phi_v^*\rangle$ are the excited configurations over the respective $|\Phi_0\rangle$ and $|\Phi_v\rangle$ DHF wave functions, and $E_v^{(k)} = \langle\Phi_v|V_{es}(1 + \Omega_0^{(k-1)} + \Omega_v^{(k-1)})|\Phi_v\rangle$ is the k^{th} order energy of the $|\Psi_v\rangle$ state.

After obtaining amplitudes of the MBPT operators, the g_j factors are calculated using the expression

$$\langle O \rangle = \frac{\langle\Psi_v|O|\Psi_v\rangle}{\langle\Psi_v|\Psi_v\rangle}, \quad (18)$$

where O stands for the respective \mathcal{M} and $\Delta\mathcal{M}$ operators for the evaluations of the g_j^D and Δg_j^Q contributions.

In the similar framework and using the exponential ansatz of RCC theory, atomic wave functions of the considered states with the respective valence orbitals are expressed as

$$|\Psi_v\rangle = e^T \{1 + S_v\}|\Phi_v\rangle, \quad (19)$$

where T and S_v are the RCC operators that excite electrons from $|\Phi_0\rangle$ and $|\Phi_v\rangle$, respectively. We have approximated RCC theory to only the singles and doubles excitations (CCSD method). The single and double excitation processes carried out by these RCC operators are described by denoting these operators using the subscripts 1 and 2, respectively, as

$$T \simeq T_1 + T_2 \quad \text{and} \quad S_v \simeq S_{1v} + S_{2v}. \quad (20)$$

The amplitudes of these operators are evaluated by solving the equations

$$\langle\Phi_0^*|\overline{H}_N|\Phi_0\rangle = 0 \quad (21)$$

and

$$\langle\Phi_v^*|(\overline{H}_N - \Delta E_v)S_v|\Phi_v\rangle = -\langle\Phi_v^*|\overline{H}_N|\Phi_v\rangle, \quad (22)$$

where $|\Phi_0^*\rangle$ and $|\Phi_v^*\rangle$ are excited up to doubles, $\overline{H}_N = (H_N e^T)_l$ represents for the linked terms only with the normal order Hamiltonian $H_N = H - \langle\Phi_0|H|\Phi_0\rangle$ and ΔE_v is the attachment energy for the state $|\Psi_v\rangle$, which is determined by

$$\Delta E_v = \langle\Phi_v|\overline{H}_N\{1 + S_v\}|\Phi_v\rangle. \quad (23)$$

To investigate the roles of the electron correlation effects through the non-linear terms in the RCC theory, we also perform calculations considering only linear terms in the singles and doubles approximation in this theory (which is termed as LCCSD method). In this approximation, it yields

$$|\Psi_v\rangle \approx \{1 + T + S_v\}|\Phi_v\rangle, \quad (24)$$

$$\overline{H}_N \approx H_N + H_N T \quad (25)$$

and

$$\overline{H}_N S_v \approx H_N + H_N T + H_N S_v. \quad (26)$$

After obtaining amplitudes of the RCC operators, the expectation values as in Eq. (18) are evaluated by

$$\frac{\langle\Psi_v|O|\Psi_v\rangle}{\langle\Psi_v|\Psi_v\rangle} = \frac{\langle\Phi_v|\{1 + T^\dagger + S_v^\dagger\}O\{1 + T + S_v\}|\Phi_v\rangle}{\langle\Phi_v|\{1 + T^\dagger + S_v^\dagger\}\{1 + T + S_v\}|\Phi_v\rangle} \quad (27)$$

in the LCCSD method and

$$\frac{\langle\Psi_v|O|\Psi_v\rangle}{\langle\Psi_v|\Psi_v\rangle} = \frac{\langle\Phi_v|\{1 + S_v^\dagger\}e^{T^\dagger}Oe^T\{1 + S_v\}|\Phi_v\rangle}{\langle\Phi_v|\{1 + S_v^\dagger\}e^{T^\dagger}e^T\{1 + S_v\}|\Phi_v\rangle} \quad (28)$$

in the CCSD method. Clearly, the expression for the LCCSD method gives rise finite number of terms like in

TABLE II: Demonstration of trends of the calculated g_j^D values in various relativistic methods using the DC Hamiltonian. Relativistic corrections from the CCSD method and contributions from the important triple excitations are given separately. Contributions to Δg_j^Q at the DHF and CCSD method are also listed with the DC Hamiltonian. Accounting both the g_j^D and Δg_j^Q values, the net g_j values are estimated in the DHF and CCSD methods to compare them with the available experimental results in the $4s^2 S_{1/2}$ and $3d^2 D_{5/2}$ states.

	$4s^2 S_{1/2}$	$3d^2 D_{3/2}$	$3d^2 D_{5/2}$	$4p^2 P_{1/2}$	$4p^2 P_{3/2}$
	DC contributions at the DHF method				
g_j^D	1.999953	0.799922	1.199917	0.666636	1.333308
Δg_j^Q	0.002320	-0.000464	0.000464	-0.000773	0.000773
Net g_j	2.002273	0.799458	1.200381	0.665863	1.334081
	DC contributions to g_j^D				
MBPT(2)	1.999551	0.798641	1.197217	0.666457	1.333004
MBPT(3)	1.999997	0.782330	1.186208	0.669819	1.333903
LCCSD	1.996755	0.800997	1.197612	0.666674	1.332832
	CCSD results to g_j^D				
DC	2.000654	0.799512	1.200430	0.666685	1.333521
+Breit	2.000651	0.799550	1.200438	0.666689	1.333522
+QED	2.000651	0.799550	1.200438	0.666689	1.333522
+Breit+QED	2.000650	0.799550	1.200438	0.666690	1.333522
+Triples	1.999946	0.799019	1.199876	0.666409	1.333088
Δg_j^Q	0.002321	-0.000465	0.000465	-0.000773	0.000773
Net g_j	2.002267	0.79855	1.200341	0.665636	1.333861
Experiment	2.00225664(9) [7]		1.2003340(25) [1]		

the MBPT(2) and MBPT(3) methods. However, the expression for the CCSD method has two non-terminating series in the numerator and denominator as $e^{T^\dagger} O e^T$ and $e^{T^\dagger} e^T$ respectively. These non-truncative series give a large number of non-linear terms corroborating a large space of CSFs belonging to higher level of excitations. To account for contributions from both the non-truncative series, we adopt iterative procedures. This is done by performing calculations through intermediate steps, in which we compute and store first the $O + OT + T^\dagger O + T^\dagger OT$ terms from $e^{T^\dagger} O e^T$ and $1 + T^\dagger T$ terms from $e^{T^\dagger} e^T$. Then, we operate a T operator and subsequently by a T^\dagger operator on the above intermediate calculations and replace them as the new intermediate calculations. This procedure is repeated till we attain contributions up to 10^{-8} precision level convergence in the values from the higher non-linear terms.

As we shall see, the correlation effects coming through the CCSD terms give much larger magnitudes to the g_j factors than the available experimental values for the ground [7] and $3d^2 D_{5/2}$ [1] states of Ca^+ , even though this method was proven to give reasonably accurate results for a number of properties in the considered ion as stated in Introduction. To find out how the higher level excitations would circumvent this to bring back the results close to the experimental values, we define RCC operators in a perturbative framework to account for contri-

butions from the important triply excited configurations from both $|\Phi_0\rangle$ and $|\Phi_v\rangle$ as

$$T_3^{\text{pert}} = \frac{1}{6} \sum_{abc,pqr} \frac{(H_N T_2)_{abc}^{pqr}}{\epsilon_a + \epsilon_b + \epsilon_c - \epsilon_p - \epsilon_q - \epsilon_r} \quad (29)$$

and

$$S_{3v}^{\text{pert}} = \frac{1}{4} \sum_{ab,pqr} \frac{(H_N T_2 + H_N S_{2v})_{abv}^{pqr}}{\Delta E_v + \epsilon_a + \epsilon_b - \epsilon_p - \epsilon_q - \epsilon_r}, \quad (30)$$

where $\{a, b, c\}$ and $\{p, q, r\}$ represent for the occupied and virtual orbitals, respectively, and ϵ s are their single particle orbital energies. Contributions from the T_3^{pert} and S_{3v}^{pert} operators to the g_j factors are estimated using Eq. (28) considering them as part of the T and S_v operators. In this approach, we evaluate extra terms as $T_2^\dagger O T_3^{\text{pert}}$, $T_2^\dagger O S_{3v}^{\text{pert}}$, $S_{2v}^\dagger O S_{3v}^{\text{pert}}$, $S_{1v}^\dagger T_2^\dagger O S_{3v}^{\text{pert}}$, $T_3^{\text{pert}\dagger} O T_3^{\text{pert}}$, $S_{3v}^{\text{pert}\dagger} O S_{3v}^{\text{pert}}$, and their complex conjugate (c.c.) terms. These terms are computationally very expensive and give more than 500 Goldstone diagrams, but found to be crucial in achieving reasonably accurate results compared to the available experimental values.

TABLE III: Contributions from individual CCSD terms to the g_j^D values in the $4s^2S_{1/2}$, $3d^2D_{3/2}$, $3d^2D_{5/2}$, $4p^2P_{1/2}$, and $4p^2P_{3/2}$ states. Contributions quoted as “Extra” and “Norm” are obtained from the rest of the non-linear terms of the CCSD method that are not listed here and corrections due to normalization of the wave functions, respectively. Values up to only the sixth decimal place are given and those values are finite but contribute below 10^{-6} precision level are quoted as ~ 0.0 . Unusually large contributions coming from the correlation effects are highlighted by quoting them in bold. We have also underlined the “Extra” contribution to the $3d^2D_{5/2}$ state to draw its attention for its very large value.

RCC terms	$4s^2S_{1/2}$	$3d^2D_{3/2}$	$3d^2D_{5/2}$	$4p^2P_{1/2}$	$4p^2P_{3/2}$
O	1.999953	0.799922	1.199917	0.666636	1.333308
$OT_1+c.c.$	~ 0.0	0.0	0.0	~ 0.0	~ 0.0
$T_1^\dagger OT_1$	0.000001	0.0	0.0	0.000003	0.000007
$T_1^\dagger OT_2+c.c.$	~ 0.0	0.0	0.0	~ 0.0	~ 0.0
$T_2^\dagger OT_2$	-0.000912	-0.006104	-0.009066	-0.000234	-0.000525
$OS_{1v}+c.c.$	-0.000009	-0.000016	-0.000018	-0.000003	-0.000005
$OS_{2v}+c.c.$	0.000001	-0.000004	0.000005	-0.000003	-0.000003
$T_1^\dagger OS_{2v}+c.c.$	-0.000984	-0.001526	-0.002282	-0.000144	-0.000284
$T_2^\dagger OS_{2v}+c.c.$	~ 0.0	~ 0.0	~ 0.0	~ 0.0	~ 0.0
$S_{1v}^\dagger OS_{1v}$	0.005060	0.009181	0.013637	0.001606	0.003169
$S_{1v}^\dagger OS_{2v}+c.c.$	~ 0.0	~ 0.0	0.000001	~ 0.0	~ 0.0
$S_{2v}^\dagger OS_{2v}$	0.016159	0.018597	0.000008	0.004210	0.007462
$T_2^\dagger OT_3^{pert}+c.c.$	~ 0.0	~ 0.0	~ 0.0	~ 0.0	~ 0.0
$S_{2v}^\dagger OT_3^{pert}+c.c.$	0.0	0.0	0.0	0.0	0.0
$T_2^\dagger OS_{3v}^{pert}+c.c.$	-0.001650	-0.000907	-0.001104	-0.000440	-0.000804
$S_{2v}^\dagger OS_{3v}^{pert}+c.c.$	~ 0.0	~ 0.0	~ 0.0	~ 0.0	~ 0.0
$T_3^{pert\dagger} OT_3^{pert}$	0.000136	0.000159	0.000235	0.000050	0.000098
$S_{3v}^{pert\dagger} OS_{3v}^{pert}$	0.000728	0.000238	0.000366	0.000130	0.000255
$S_{1v}^\dagger T_2^\dagger OS_{3v}^{pert}+c.c.$	-0.000076	-0.000021	-0.000007	-0.000021	-0.000038
Extra	0.002951	-0.001207	<u>0.026959</u>	-0.000313	0.000411
Norm	-0.021567	-0.019331	-0.028730	-0.005073	-0.010019

IV. RESULTS AND DISCUSSION

In order to gauge correctness of the wave functions obtained by employing many-body methods at different levels of approximations, we first present electron attachment energies to the considered states of Ca^+ in Table I and compare them with the experimental values listed in the National Institute of Science and Technology (NIST) database [30]. We consider only the $4s^2S_{1/2}$, $3d^2D_{3/2}$, $3d^2D_{5/2}$, $4p^2P_{1/2}$ and $4p^2P_{3/2}$ states of Ca^+ as the representative states with different angular momentum and parity for our investigation. As can be seen from this table, the DHF results differ significantly from the experimental values while the MBPT(2) values are larger than the experimental results. The LCCSD method does not seem to improve the calculations and give even larger values than the MBPT(2) results. However, the CCSD method brings down these results close to the experimental values. Corrections from the Breit and QED interactions are given separately in the same table from the CCSD method. They are also estimated by including both these interactions simultaneously. In this case, we find sum of the individual corrections and simultaneous account of these corrections, quoted as Breit+QED

in the above table, give almost the same contributions. In our earlier work on the Cs atom, we had found similar behavior for the attachment energies but trends were exhibiting differently in the evaluation of the transition properties [27]. Nevertheless, the higher order relativistic corrections are also removing slightly the discrepancies among the CCSD results and experimental values of the energies. It may be possible that the omitted contributions from the triple excitations improve the CCSD values further.

After understanding the role of the electron correlation effects in the evaluation of the energies, we present the calculated g_j values of the $4s^2S_{1/2}$, $3d^2D_{3/2}$, $3d^2D_{5/2}$, $4p^2P_{1/2}$ and $4p^2P_{3/2}$ states of Ca^+ in Table II from a number of methods approximating at different levels. This also includes all the methods that were considered for evaluating energies along with the MBPT(3) method, which involves energies from the MBPT(2) method. To highlight how the correlation effects propagate in these methods, we present results systematically from lower to all order LCCSD and CCSD methods. We present both the g_j^D and Δg_j^Q results from the DHF method in the beginning to appraise beforehand about how much the electron correlation effects may render to the contributions for yielding results close to the experimental values

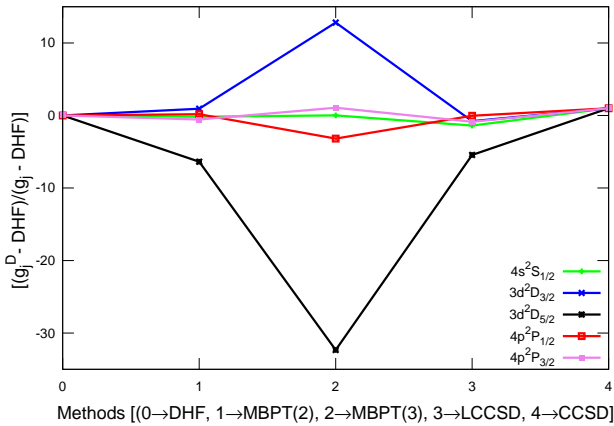


FIG. 1: Trends of electron correlation effects among the $4s\ ^2S_{1/2}$, $3d\ ^2D_{3/2}$, $3d\ ^2D_{5/2}$, $4p\ ^2P_{1/2}$ and $4p\ ^2P_{3/2}$ states for the evaluation of g_j^D values in Ca^+ . We plot the relative $(g_j^D - \text{DHF})/(g_j - \text{DHF})$ values to highlight the roles of correlation effects through different many-body methods. We consider values from the DHF, MBPT(2), MBPT(3), LCCSD and CCSD methods in a sequence referring them in the X-axis in an arbitrary unit distance.

in the measured states. In case, we are able to achieve results agreeing with the experimental values for some states then it may be possible to predict these values for other states using the employed many-body methods where measurements are not carried out. From the analysis of behavior of the correlation effects in the determination of the attachment energies, it was obvious to us that there were large differences between the calculations obtained using the DHF method and the experimental values. When we compare the net g_j values of the ground and $3d\ ^2D_{5/2}$ states, after adding up the g_j^D and Δg_j^Q values, with the experimental results [1, 7] quoted at the end of the above table, it gives an impression that the electron correlation effects may not play strong roles for attaining calculated values matching with the experimental results. So it is natural to assume that employment of a lower order method can suffice the purpose. In the experimental paper on the ground state result, the authors have also presented theoretical results by carrying out a rigorous calculation employing the MCDF method [7]. It is demonstrated there that a very large configurational space was required to attain results matching with their measured value. It was also highlighted in that work that the Breit interaction contribution was essential in achieving high precision theoretical result.

As we move on, we shall explain the reasons why we shall not be able to achieve very high precision results by employing RCC theory in the CCSD method approximation. Thus, we do not prefer to present the calculated values of the g_j factors beyond the sixth decimal places here. Necessity of including higher level excitations through the RCC method to improve these results

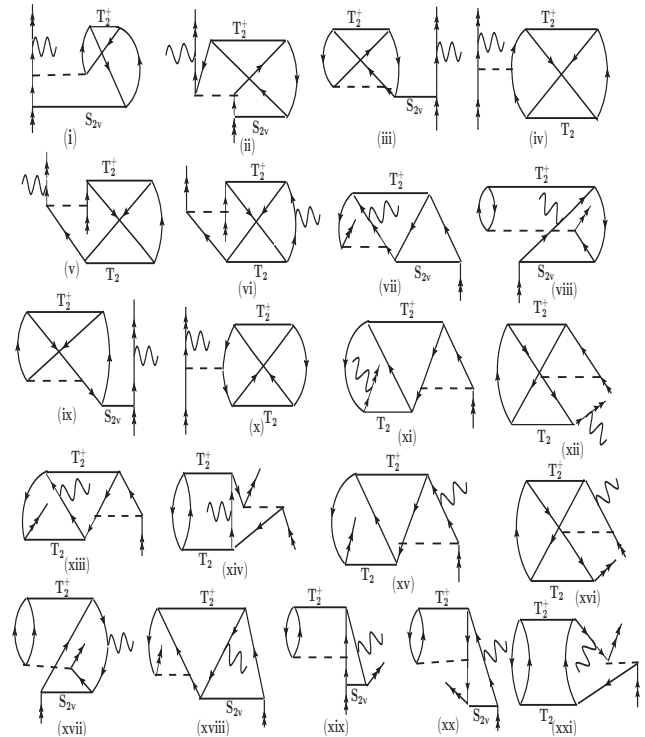


FIG. 2: Some of the important contributing Goldstone diagrams appearing through the $T_2^+ OS_{3v}^{pert}$ RCC term. Lines going up and down represent for the virtual and occupied orbitals of Ca^+ . Lines with double arrows correspond to the valence orbital, dotted horizontal line means Coulomb interaction and solid horizontal lines correspond to the all order Coulomb interactions appearing through the T_2 and S_{2v} operators.

further are demonstrated by investigating contributions from the leading order triple excitation contributions involving the core and valence orbitals at the MBPT(3) method and in the perturbative approach using the RCC operators as defined in Eqs. (29) and (30). We have also quoted corrections to g_j^D from the Breit and QED corrections considering them separately and also considering both the interactions together. The estimated Δg_j^Q corrections from the CCSD method are also listed explicitly. Signs of these corrections are not the same for all the states owing to the $\kappa_f + \kappa_i - 1$ factor in Eq. (11). It is obvious from Table II that our CCSD results do not look very impressive when compared with the available experimental values. However the important point to be noted from this work is on the trends of the results starting from the DHF method to the CCSD method, which shows how values are vacillating from one method to another in different states.

Since the differences among the values of the g_j^D factors among various methods are very small, the role of electron correlation effects are not realized distinctly. To make it pronounced, we plot the $(g_j^D - \text{DHF})/(g_j - \text{DHF})$

values considering g_j^D values from different methods in Fig. 1 for all the states. It highlights the trends of the electron correlation effects incorporated through these methods. As can be seen from this figure, the correlation contributions do not follow definite trends and they are quite significant in view of achieving high precision values. Also, we give contributions to the g_j^D values for all the considered states from the individual terms of the CCSD method including the terms including the perturbed triple excitations operators in Table III. This is to notify how some of the higher order terms in the all order perturbative method contribute larger than the lower order RCC terms. The DHF value gives here the largest contribution as it includes the Dirac g_D value. It has been found in the earlier studies on hyperfine structure constants and quadrupole moments of atomic states in $^{43}\text{Ca}^+$ using the RCC method [11] that after the DHF value, the dominant contributions come from the OS_{1v} and OS_{2v} terms along with their c.c. terms due to the electron correlation effects. It to be kept in mind that the OS_{1v} term accounts for the lowest order electron pair-correlation effects, while the OS_{2v} term incorporates the lowest order electron core-polarization effects in the RCC framework [31, 32]. The other terms encompass higher order correlation effects due to non-linear in RCC operators. Hence, it is generally anticipated that contributions from these non-linear terms are relatively smaller compared to the above two terms. However, we find in this case that many of the non-linear terms are giving much larger contributions, almost by an order, than the lower order RCC terms. Significantly contributing correlation effects are quoted in bold in the above table. Those non-linear terms from the CCSD method, which are not listed in the above table, their total contributions are given as ‘‘Extra’’. It is obvious from the above table that these contributions are quite large, especially in the $3d^2D_{5/2}$ state which has been underlined. This suggests the core correlation contributions appearing through the T operators in the non-linear terms play active roles in the evaluation of the g_j^D values. Thus, it testifies that consideration of a perturbative method would completely fail to estimate the g_j factors accurately in an atomic system. We had also seen in Table II that contributions from the estimated triple excitations through the perturbed RCC operators are the decisive factors to attain the results close to the available experimental values. Following the perturbative analysis, it can be perceived that the $T_2^\dagger OT_3^{pert}$, $S_{2v}^\dagger OT_3^{pert}$, $T_2^\dagger OT_3^{pert}$ and $S_{2v}^\dagger OS_{3v}^{pert}$ RCC terms account for the lowest order terms involving the triply excited perturbed excitation operators. Since the S_{3v}^{pert} operator involves the valence orbital, the term including this operator usually gives the larger contributions than the counter terms with the T_3^{pert} operator. But comparison between the contributions obtained through the $T_2^\dagger OT_3^{pert}$, $S_{2v}^\dagger OS_{3v}^{pert}$ and $S_{3v}^{pert\dagger} OS_{3v}^{pert}$ terms quoted in Table III suggest that the correlation contributions do not manifest this trend. An-

alyzing in terms of level of excitations associated with all these operators, as defined in Ref. [19], it can be understood that the Goldstone diagrams involving the particle-particle and hole-hole excitations through the M operator are the important physical processes and the hole-particle and particle-hole excitations do not play much role in determining the g_j^D values.

Again, we have observed that similar types of Goldstone diagrams attribute completely different trends of correlation effects at the lowest order and all order methods. To demonstrate it more prominently, we find out the leading order contributing diagrams from the $T_2^\dagger OT_3^{pert}$ and $S_{2v}^\dagger OS_{3v}^{pert}$ RCC terms and compare contributions from these diagrams with their counter lowest order Goldstone diagrams appearing through the MBPT(3) method. We have shown some of these diagrams in Fig. 2 and quote their contributions in Table IV from the MBPT(3) and RCC methods. As can be seen from this table, there are huge differences in some of the results obtained at the MBPT(3) method and at the level of RCC calculations. We have also quoted some contributions in bold to bring to the attention on the unusually large contributions at the lower and all order level calculations. Again, it is obvious from this table that some diagrams contribute predominantly to the lower angular momentum states while other diagrams contribute significantly in higher angular momentum states. Some changes in the correlation trends are also observed among the states belonging to different parities.

Nonetheless, unusually large contributions arising through the perturbed triple excitation RCC operators implies that RCC theory in the CCSD method approximation is not capable of producing precise values of the g_j factors in Ca^+ . Also, larger contributions arising through some of the non-linear terms than the linear terms in the CCSD method suggests that consideration of full triple excitations may be imperative to achieve g_j factors below the 10^{-6} precision level. Moreover, either estimating the $g_j^D - g_D$ value as in Ref. [15] or developments of alternative RCC theories, such as bi-orthogonal RCC theory [19], avoiding appearance of non-truncative series as in Eq. (28) to determine the g_j factor of a state in this ion would be inevitable.

V. CONCLUSION

We have employed a number of relativistic many-body methods to investigate roles of the electron correlation effects in the determination of the g_j factors of the first five low-lying atomic states in the singly charged calcium ion. To validate these methods, we first present the electron attachment energies by employing these methods and compare them against the experimental values listed in the National Institute of Science and Technology database. This demonstrates gradual improvement of accuracies in the results from lower many-body methods to all order relativistic coupled-cluster method with the

TABLE IV: Contributions to g_j^D values of different states from the individual diagrams shown in Fig. 2. Values are given after multiplying with 10^3 to highlight their contributions prominently and those values which are unusually large are quoted in bold. This clearly demonstrates importance of considering an all order perturbative method for the determination of the g_j factors in the atomic systems.

Diagrams	$4s^2S_{1/2}$		$3d^2D_{3/2}$		$3d^2D_{5/2}$		$4p^2P_{1/2}$		$4p^2P_{3/2}$	
	MBPT(3)	RCC	MBPT(3)	RCC	MBPT(3)	RCC	MBPT(3)	RCC	MBPT(3)	RCC
Fig. 2(i)	0.4425	0.9141	0.3852	0.8401	0.5758	1.2575	0.0874	0.1820	0.1732	0.3613
Fig. 2(ii)	-0.1108	-0.1652	-0.1864	-0.2811	-0.2800	-0.4228	-0.03306	-0.0565	-0.0668	-0.1143
Fig. 2(iii)	0.2023	0.3247	0.4086	0.6099	0.6107	0.9123	0.0426	0.0742	0.0848	0.1477
Fig. 2(iv)	12.6380	20.5263	7.7036	12.2213	11.5434	18.3284	3.5011	5.5020	6.9796	10.9658
Fig. 2(v)	-0.2017	-0.2983	-0.5771	-0.9463	-0.8665	-1.4226	-0.03446	-0.0488	-0.0689	-0.9758
Fig. 2(vi)	-0.2015	-0.2976	0.7874	1.3197	0.0436	0.0882	0.0518	0.0766	-0.0256	-0.0344
Fig. 2(vii)	-0.0913	-0.1323	0.0596	0.0845	-0.0843	-0.1372	~ 0.0	~ 0.0	-0.0385	-0.6697
Fig. 2(viii)	0.2316	0.3907	-0.1859	-0.2984	0.0250	0.0662	~ 0.0	0.0271	0.0939	0.1601
Fig. 2(ix)	-0.2204	-0.3402	-0.4415	-0.6485	-0.6600	-0.9701	-0.0459	-0.0770	-0.0915	-0.1533
Fig. 2(x)	-12.7009	-20.6074	-7.8297	-12.3756	-11.7321	-18.5594	-3.5141	-5.5182	-7.0057	-10.9981
Fig. 2(xi)	0.1408	0.2022	0.5118	0.8461	0.7691	1.2728	0.0270	0.0350	0.0544	0.0709
Fig. 2(xii)	0.1322	0.1910	0.4986	0.8294	0.74897	1.2473	0.0256	0.0332	0.0516	0.0672
Fig. 2(xiii)	0.1403	0.2013	-0.8225	-1.3819	-0.1216	-0.2143	-0.0442	-0.0620	0.0183	0.0213
Fig. 2(xiv)	-0.4488	-0.6347	~ 0.0	0.0536	-0.9322	-1.2610	-0.0238	-0.0225	-0.1680	-0.2248
Fig. 2(xv)	0.1409	0.2023	0.5057	0.8341	0.7651	1.2648	1.2648	0.0315	0.05293	0.0692
Fig. 2(xvi)	0.1323	0.1911	0.4847	0.8071	0.7399	1.2323	0.0202	0.0268	0.0489	0.0641
Fig. 2(xvii)	-0.2309	-0.4032	0.1170	0.1908	-0.0707	-0.1466	0.0206	0.0371	-0.0793	-0.1334
Fig. 2(xviii)	0.0914	0.1369	-0.0665	-0.1048	0.0801	0.1306	-0.0237	-0.0471	0.0294	0.0501
Fig. 2(xix)	0.0962	0.1688	~ 0.0	-0.0180	0.0496	0.0379	-0.0289	-0.0342	-0.0121	~ 0.0
Fig. 2(xx)	~ 0.0	0.2768	~ 0.0	~ 0.0	0.8479	1.2160	~ 0.0	-0.0553	~ 0.0	0.0784
Fig. 2(xxi)	0.4482	0.6543	-0.1303	-0.1868	0.8479	1.2160	~ 0.0	~ 0.0	0.1536	0.2175

singles and doubles approximation. However, when these methods are employed for the determination of the g_j factors of the considered atomic states, the trends of the correlation effects were found to be very peculiar in nature. In fact, the results obtained employing the mean-field theory in the Dirac-Hartree-Fock approach are found to be in better agreement with the experimental values than the lower-order many-body perturbation theories and relativistic coupled-cluster theory with linear terms approximation. We also found that triple excitation contributions are the decisive factors in achieving very precise values for the g_j factors and their contributions through the lower order and all order correlation effects behave completely different. Nonetheless, the overall observation from this study is that it is very challenging to attain high accuracy g_j factors in many-electron systems by employing a truncated many-body method as the contributions from the electron correlation effects do not converge with the higher order approximations. Thus, it is reliable to determine the $g_j - g_D$ value instead of the net g_j value of an atomic state. Also, it is imperative to develop more

powerful relativistic many-body methods circumventing the problem of appearing non-truncative series so that trends of the correlation effects can be systematically investigated and calculations can be improved gradually in the determination of the g_j factors in a many-electron atomic system. Since unique correlation effects are associated with the determination of g_j factors, it suggests us that capable of a relativistic many-body method can be indeed scrutinized by producing high precision values for these factors in heavy atomic systems. This test would be of immense interest in a number of applications such as investigating parity non-conservation and frequency standard studies in atomic systems more reliably.

Acknowledgement

Computations were carried out using the Vikram-100TF HPC cluster at the Physical Research Laboratory, Ahmedabad, India.

[1] M. Chwalla, J. Benhelm, K. Kim, G. Kirchmair, T. Monz, M. Riebe, P. Schindler, A. S. Villar, W. Hänsel, C. F. Roos, R. Blatt, M. Abgrall, G. Santarelli, G. D.

Rovera, and Ph. Laurent, Phys. Rev. Lett. **102**, 023002 (2009).

[2] Y. Huang, J. Cao, P. Liu, K. Liang, B. Ou, H. Guan, X.

- Huang, T. Li, and K. Gao, Phys. Rev. A **85**, 030503(R) (2012).
- [3] M. Riebe, H. Häffner, C. F. Roos, W. Hänsel, J. Benhelm, G. P. T. Lancaster, T. W. Körber, C. Becher, F. Schmidt-Kaler, D. F. V. James, and R. Blatt, Nature **429**, 734 (2004).
- [4] T.P. Harty, D.T.C. Allcock, C.J. Ballance, L. Guidoni, H.A. Janacek, N.M. Linke, D.N. Stacey, and D.M. Lucas, Phys. Rev. Lett. **113**, 220501 (2014).
- [5] C.J. Ballance, T.P. Harty, N.M. Linke, M.A. Sepiol, and D.M. Lucas, Phys. Rev. Lett. **117**, 060504 (2016).
- [6] T. Pruttivarasin, M. Ramm, S. G. Porsev, I. I. Tupitsyn, M. S. Safronova, M. A. Hohensee and H. Häffner, Nature **517**, 592 (2015).
- [7] G. Tommaseo, T. Pfeil, G. Revalde, G. Werth, P. Indelicato, and J.P. Desclaux, Eur. Phys. J. D **25**, 113 (2003).
- [8] W. M. Itano, Phys. Rev. A **73**, 022510 (2005).
- [9] B. K. Sahoo, Md. R. Islam, B. P. Das, R. K. Chaudhuri, and D. Mukherjee, Phys. Rev. A **74**, 062504 (2006).
- [10] D. Jiang, B. Arora, and M. S. Safronova, Phys. Rev. A **78**, 022514 (2008).
- [11] B. K. Sahoo, Phys. Rev. A **80**, 012515 (2009).
- [12] M. S. Safronova and U. I. Safronova, Phys. Rev. A **83**, 012503 (2011).
- [13] Y.-B. Tang, H.-X. Qiao, T.-Y. Shi, and J. Mitroy Phys. Rev. A **87**, 042517 (2013).
- [14] C. Shi, F. Gebert, C. Gorges, S. Kaufmann, W. Nörtershuser, B. K. Sahoo, A. Surzhykov, V. A. Yerokhin, J. C. Berengut, F. Wolf, J. C. Heip, P. O. Schmidt, Appl. Phys. B **123**, 2 (2017).
- [15] E. Lindroth and A. Yennerman, Phys. Rev. A **47**, 961 (1993).
- [16] A. V. Volotka, D. A. Glazov, V. M. Shabaev, I. I. Tupitsyn, G. Plunien, Phys. Rev. Lett. **112**, 253004 (2014).
- [17] V. M. Shabaev, D. A. Glazov, G. Plunien, A. V. Volotka, J. Phys. Chem. Ref. Data **44**, 031205 (2015).
- [18] K. T. Cheng and W. J. Childs, Phys. Rev. A **31**, 2775 (1985).
- [19] I. Shavitt and R. J. Bartlett, *Many-body methods in Chemistry and Physics*, Cambridge University Press, Cambridge, UK (2009).
- [20] A. Szabo and N. Ostlund, *Modern Quantum Chemistry*, Dover Publications, Inc., Mineola, New York, First edition (revised), 1996.
- [21] C. Sur, K. V. P. Latha, B. K. Sahoo, R. K. Chaudhuri, B. P. Das, and D. Mukherjee, Phys. Rev. Lett. **96**, 193001 (2006).
- [22] B. K. Sahoo, B. P. Das, and D. Mukherjee, Phys. Rev. A **79**, 052511 (2009).
- [23] J. J. Sakurai, *Advanced Quantum Mechanics*, Addison-Wesley Publishing Company, Virginia, USA, 1967.
- [24] A. Czarnecki, U. D. Jentschura, K. Pachucki, and V. A. Yerokhin, Can. J. Phys. **83**, 1 (2005).
- [25] A. J. Akhiezer and V. B. Berestetskii, *Quantum Electrodynamics*, Interscience, New York, 1965, Chap. 8, Sec. 50.2.
- [26] D. K. Nandy and B. K. Sahoo, Phys. Rev. A **90**, 050503(R) (2014).
- [27] B. K. Sahoo, Phys. Rev. A **93**, 022503 (2016).
- [28] V. V. Flambaum and J. S. M. Ginges, Phys. Rev. A **72**, 052115 (2005).
- [29] I. Lindgren and J. Morrison, *Atomic Many-Body Theory*, Second Edition, Springer-Verlag, Berlin, Germany (1986).
- [30] http://physics.nist.gov/PhysRefData/ASD/levels_form.html
- [31] B. K. Sahoo, G. Gopakumar, H. Merlitz, R. K. Chaudhuri, B. P. Das, U. S. Mahapatra and D. Mukherjee, Phys. Rev. A **68**, 040501(R) (2003).
- [32] B. K. Sahoo, S. Majumder, R. K. Chaudhuri, B. P. Das and D. Mukherjee, J. Phys. B **37**, 3409 (2004).